Mean field Ehrenfest quantum/classical simulation of vibrational energy relaxation in a simple liquid

Günter Käb*
Max-Planck-Institut für Biophysikalische Chemie, Am Fassberg 11, D-37077 Göttingen, Germany
(Received 27 March 2002; published 15 October 2002)

We give a detailed account of the statistical mechanical properties of the mean field Ehrenfest quantum/classical method as applied to liquid phase vibrational energy transfer using a simple harmonic oscillator model Hamiltonian. Depending on the shape of the initial quantum wave packet, a (partial) breakdown of detailed balance is observed, where the frictional response of the classical bath is only correlated to quasiclassical features of the evolving quantum state, i.e., a classical-like fluctuation-dissipation theorem holds. Only in the case of a coherent initial state (minimum uncertainty wave packet) does the mean field method produce physically meaningful results, namely, exponential relaxation ($\tau = \tau_{cl}$) towards a quasiclassical equilibrium.

DOI: 10.1103/PhysRevE.66.046117 PACS number(s): 82.20.−w, 05.30.−d

I. INTRODUCTION

Mixed quantum/classical or semiclassical molecular dynamics methods have recently been the subject of renewed and increasing interest especially in the field of condensed phase chemical dynamics [1–8]. Basically, this arises from the fact that many important chemical processes involve the motion of light particles such as electrons or protons or afford the inclusion of quantum effects for some degrees of freedom, while at the same time a full quantum treatment of a many particle system is impossible. Typical examples are electronically nonadiabatic processes such as internal conversion [9] or photodissociation in liquids and solid matrices [6,10] or proton/hydrogen transfers in chemistry and biology [4,5]. Vibrational energy transfer [VET, vibrational energy relaxation (VER)] is an elementary process of fundamental importance in chemical dynamics where quantum effects may also become important due to the non-negligible zero point energy of high frequency vibrations and the discreteness of their energy spectra. Moreover, since a quantum oscillator can explore classically forbidden regions of the potential energy function—this is often called dynamical tunneling [11]—, the exact quantum rate of relaxation may become larger than the rate obtained from a purely classical treatment, despite the discreteness of the quantum energy scale.

Semiclassical methods [8] are usually derived from the Feynman path integral and, at the highest level, treat all degrees of freedom on an equal footing, namely, semiclassical mechanics. However, at present these methods are limited to short times below and up to $\approx$1 ps, while vibrational relaxation in the condensed phase takes place on picosecond to nanosecond time scales and beyond.

Hybrid quantum/classical molecular dynamics, hereafter denoted by the acronym QCMD, is distinct from semiclassical treatments, in that it involves the propagation of a quantum wave packet for the quantum degrees of freedom (DOF), whereas classical equations of motion are solved for the remaining DOF. Quantum and classical equations of motion are solved in a self-consistent manner. Mixed quantum/classical methods have the advantage that the stability of integration schemes allows for longer simulation times up to hundreds of picoseconds, although the shortest time step dictated by the time dependence of quantum probability amplitudes is typically significantly smaller than in a corresponding purely classical treatment.

When applying QCMD, one always has to keep in mind that these methods involve unavoidable approximations, the validity of which must be checked for the specific physical system under investigation. This is usually done by benchmarking against fully correlated quantum simulations for small to moderately large systems. However, the number of model systems mimicking the effects of a condensed phase environment, which can be solved exactly in a quantum treatment, is limited, e.g., Ref. [12], and these models often do not contain anharmonic interactions typical for a liquid solution, as employed in the present study. Here we use instead the assumption that the quantum rate of energy relaxation may be estimated from a knowledge of the classical rate as described later.

QCMD methods may be divided into two categories depending on the level of approximation especially pertaining to the degree of correlation between quantum and classical subsystems. The lowest level of theory is represented by the so-called mean field Ehrenfest (MF) or classical path method [2,5], which can rigorously be derived from the single-configuration time-dependent self-consistent field (TDSCF) approximation [6,7,13,14]. As a result, it suffers from the same approximations as involved in the derivation of TDSCF, namely, the (partial) neglect of correlation between subsystems described by separate lower-dimensional wave functions. While the TDSCF and MF methods are applicable to situations with small coupling between subsystems or where the interaction between subsystems is of an average type, mean field performs poorly for systems with large coupling and strong dependence of classical forces on the quantum state [15]. In general terms, the drawback of the mean field approach arises from the property that the motion of classical degrees of freedom is not correlated to the full probability density or density matrix of the quantum DOF, but only to an expectation value calculated there from, namely,

*FAX: +49 (0)551/201-1006. Email address: gkaeb@gwdg.de

an average Hellmann-Feynman-type force.

The molecular dynamics with electronic transitions method [16], widely known as *surface hopping* (SH), has been specifically designed to handle this correlation problem, and represents the second class of QCMD schemes. Various implementations of surface hopping and related approaches have been developed, and an extension to nonadiabatic transitions between proton states, termed molecular dynamics with quantum transitions [4,17], has been worked out. A nice review of SH and related developments may be found in Ref. [5].

In this work we apply QCMD to dissipative vibrational energy transfer in solution, where we explore the performance and statistical mechanical properties of the mean field Ehrenfest method in nonequilibrium simulations for the simple model system of a harmonic breathing sphere in a Lennard-Jones fluid at liquid density. Our main goal is to investigate the effect of different quantum initial conditions, i.e., coherent state vs delocalized eigenstate, on the dissipative redistribution of energy between the quantum oscillator and the classical solvent bath. While for electronically nonadiabatic processes the region of strong nonadiabatic coupling is often well localized in position space, in vibrational relaxation the coupling between diabatic as well as between adiabatic states is delocalized in the phase space of classical particles and therefore is nonvanishing throughout the course of a simulation. Thus, we can expect the mean field scheme to be a reasonably good starting point for investigations. However, it is to be expected that detailed balance is not treated properly [2,18] and the results obtained will depend on the shape of the evolving quantum wave packet.

The theoretical treatment of condensed phase vibrational energy transfer has a long history [19], which we shall not trace here in detail. If zero point energy effects may be neglected, a purely classical approach can be used in the context of equilibrium statistical mechanics (i) to calculate the mean energy relaxation time from the linear response theory [19,20], as well as for nonequilibrium simulations and (ii) to study in detail the dynamical evolution of energy redistribution, e.g., Refs. [21,22]. In fact, even for high frequency oscillators the overall energy relaxation may be reasonably described by a classical treatment, although unphysical zero point energy loss is unavoidable. In quantum approaches to condensed phase VER, perturbational treatments based on the linear response theory still dominate, where state-to-state transition rates may be calculated from the spectral density of classical force-force correlation functions [19,20,23]. When classical correlation functions are employed, the detailed balance constraint must be invoked explicitly. A critical consideration of the approximations involved in quantum-oscillator/classical-bath approaches has recently been given by Egorov, Rabani, and Berne [20] in the context of the perturbational approach. Only recently direct nonequilibrium QCMD simulations [23,24] and related treatments [25] of VER in solution have been reported. However, we feel that the strengths and weaknesses as well as the statistical mechanical consequences of direct nonequilibrium QCMD approaches to dissipative vibrational energy transfer in realistic solvent environments are still poorly understood. By investigating the statistical mechanical properties of the mean field QCMD scheme we hope to contribute to the development of quantum/classical simulation methodology in the context of condensed phase dissipative vibrational dynamics.

Our paper is organized as follows. In Sec. II we give a description of the mean field Ehrenfest method as derived from the TDSCF approximation. Section III describes our model Hamiltonian of a harmonic breathing sphere dissolved in a Lennard-Jones liquid and its parametrization as well as the thermodynamic conditions. We also discuss the propagation scheme used to integrate the coupled quantum/classical equations of motion and its implementation. In Sec. IV we report and discuss our results obtained from nonequilibrium simulations starting with different quantum initial states at a given mean excess vibrational energy. We also include in this section some of the theoretical considerations which could have been put into Sec. II, because they are closely tied to the emerging results. Section V concludes by summarizing our key findings.

II. THEORY

In the single-configuration TDSCF [6,13,26] approximation the full many-dimensional quantum state vector $|\Psi\rangle$ is written as a product of single-particle or single-DOF vectors $|\varphi_i\rangle$, say

$$|\Psi\rangle = |\varphi_1\rangle|\varphi_2\rangle, \tag{1}$$

and this separability is assumed to hold for all times. Insertion of Eq. (1) into the time-dependent Schrödinger equation (TDSE) together with a Hamiltonian of the form $\hat{H}=\hat{H}_1+\hat{H}_2+\hat{H}_{12}$ and multiplication from the left by $\langle\varphi_1|$ and $\langle\varphi_2|$, respectively, leads to a coupled set of one-dimensional Schrödinger equations

$$i\hbar|\dot{\varphi}_1\rangle = \hat{H}^{(1)}|\varphi_1\rangle, \quad \hat{H}^{(1)} = \langle\varphi_2|\hat{H}|\varphi_2\rangle; \tag{2}$$

$$i\hbar|\dot{\varphi}_2\rangle = \hat{H}^{(2)}|\varphi_2\rangle, \quad \hat{H}^{(2)} = \langle\varphi_1|\hat{H}|\varphi_1\rangle; \tag{3}$$

$$i\hbar|\dot{\Psi}\rangle = \{\hat{H}^{(1)}+\hat{H}^{(2)}\}|\Psi\rangle, \tag{4}$$

where we have implicity assumed that $\langle\varphi_1|\dot{\varphi}_1\rangle = \langle\varphi_2|\dot{\varphi}_2\rangle = 0$, which fixes the phases of $|\varphi_1\rangle$ and $|\varphi_2\rangle$ and guarantees that $|\varphi_1\rangle$ and $|\varphi_2\rangle$ remain normalized throughout the propagation, if normalized initially. From Eq. (4) we recognize that the time evolution of the full quantum state vector $|\Psi\rangle$ is determined by an effective Hamiltonian $\hat{H}^{(1)}+\hat{H}^{(2)}$ which differs from the exact one. In a more rigorous derivation [26], the total state vector is written as

$$|\Psi\rangle = a(t)|\varphi_1\rangle|\varphi_2\rangle, \tag{5}$$

where the complex number $a(t)$ is introduced to allow for a free choice of phases of both $|\varphi_1\rangle$ and $|\varphi_2\rangle$ at a fixed overall phase of $|\Psi\rangle$. The quantum equations of motion for $a(t)$, $|\varphi_1\rangle$, and $|\varphi_2\rangle$ are then derived from the Dirac-Frenkel variational principle [26,27],

$$\langle \delta\Psi | \left\{ \hat{H} - i\hbar \frac{\partial}{\partial t} \right\} | \Psi \rangle = 0, \tag{6}$$

resulting in

$$i\hbar \dot{a} = \langle \hat{\hat{H}} \rangle a, \tag{7}$$

$$i\hbar |\dot{\varphi}_1\rangle = \{\hat{H}^{(1)} - \langle \hat{H} \rangle\} |\varphi_1\rangle, \tag{8}$$

$$i\hbar |\dot{\varphi}_2\rangle = \{\hat{H}^{(2)} - \langle \hat{H} \rangle\} |\varphi_2\rangle, \tag{9}$$

$$i\hbar |\dot{\Psi}\rangle = \{\hat{H}^{(1)} + \hat{H}^{(2)} - \langle \hat{H} \rangle\} |\Psi\rangle. \tag{10}$$

The effective Hamiltonians for propagation of single-particle vectors $|\varphi_1\rangle$ and $|\varphi_2\rangle$ are now given by

$$\hat{H}^{(1)}_{\text{eff}}(t) \equiv \{\hat{H}^{(1)} - \langle \hat{H} \rangle\} = \{\hat{H}_1 + \langle \hat{H}_{12} \rangle_2\} - \{\langle \hat{H}_1 \rangle_1 + \langle \hat{H}_{12} \rangle_{1,2}\}, \tag{11}$$

$$\hat{H}^{(2)}_{\text{eff}}(t) \equiv \{\hat{H}^{(2)} - \langle \hat{H} \rangle\} = \{\hat{H}_2 + \langle \hat{H}_{12} \rangle_1\} - \{\langle \hat{H}_2 \rangle_2 + \langle \hat{H}_{12} \rangle_{1,2}\}. \tag{12}$$

Since the phase factors of vectors $|\varphi_i\rangle$ determined by $\{\langle \hat{H}_i \rangle_i + \langle \hat{H}_{ij} \rangle_{i,j}\}$ do not affect the time-dependent expectation values calculated from $|\varphi_i\rangle$, these terms can be omitted from the $|\varphi_i\rangle$ propagation, or in other words shifted to the time dependence of $a(t)$. Due to the TDSCF ansatz, the full correlation between single-DOF densities $\hat{\sigma}_i = \mathrm{Tr}_j\{\hat{\rho}\}$ is no longer maintained, where $\hat{\rho} = |\Psi\rangle\langle\Psi|$ is the total density operator.

We now formulate the Hamiltonian in a form more suitable to our model system as well as for deriving the mean field Ehrenfest equations of motion, namely,

$$\hat{H} = \hat{H}_S + \hat{H}_B + \hat{H}_{SB}, \quad \hat{H}_S = -\frac{\hbar^2}{2\mu} \frac{\partial^2}{\partial r^2} + U_S(r),$$

$$\hat{H}_B = -\frac{\hbar^2}{2M} \frac{\partial^2}{\partial R^2} + U_B(R),$$

$$\hat{H}_{SB} = V(r,R). \tag{13}$$

Here, the system Hamiltonian $\hat{H}_S$ corresponds to the energy of a vibrational degree of freedom denoted by r. The bath Hamiltonian $\hat{H}_B$ is the sum of kinetic and potential terms for the solvent particles, where the variable R collectively represents the positions of all bath particles $\{R_\alpha\}$ including the solute center of mass. The Schrödinger equations for $|\varphi_S\rangle$ and $|\varphi_B\rangle$ (omitting unimportant phase factors) read

$$i\hbar |\dot{\varphi}_S\rangle = \{\hat{H}_S + \langle \hat{H}_{SB} \rangle_B\} |\varphi_S\rangle,$$

$$i\hbar |\dot{\varphi}_B\rangle = \{\hat{H}_B + \langle \hat{H}_{SB} \rangle_S\} |\varphi_B\rangle.$$

For taking the classical limit of the bath equations of motion, $|\varphi_B\rangle$ is written as [5]

$$\langle R | \varphi_B \rangle \equiv \varphi_B(R,t) = A(R,t) \exp\left\{ \frac{i}{\hbar} S(R,t) \right\}, \tag{14}$$

where $A(R,t)$ and $S(R,t)$ are real functions, $A^2(R,t)$ is the quantum probability density in position space and $S(R,t)$ is the quantum analog of the classical action, the gradient of which determines the momentum. If the so-called quantum potential $Q(R,t) = -(\hbar^2/2M)\nabla_R^2 A/A$ is neglected in the equation of motion for $S(R,t)$, classical equations of motion for $R(t)$ and $p_R(t)$ are obtained,

$$\dot{R}(t) = \frac{p_R(t)}{M} \equiv v_R(t), \tag{15}$$

$$\dot{p}_R(t) = M\dot{v}_R(t) = -\nabla_R \langle \varphi_S | \hat{H}_{SB} | \varphi_S \rangle - \nabla_R H_B. \tag{16}$$

While H_B is now a classical function of positions and momenta for bath particles, $\hat{H}_{SB} = \hat{H}_{SB}[R(t)]$ is still an operator in r space, where each matrix element is a time-dependent function determined by the positions $R(t)$ of bath degrees of freedom. The time evolution of the system state vector $|\varphi_S\rangle$ is governed by the TDSE

$$i\hbar |\dot{\varphi}_S\rangle = \{\hat{H}_S + \hat{H}_{SB}[R(t)]\} |\varphi_S\rangle \equiv \hat{H}_q[R(t)] |\varphi_S\rangle. \tag{17}$$

Equations (15) through (17) are the mean field Ehrenfest quantum/classical equations of motion for a Hamiltonian of the form specified by Eq. (13). The mean field Ehrenfest or classical path method may also be derived, more transparently, from a quantum/semiclassical approximation within the TDSCF ansatz using Gaussian wave packets [2,28].

The classical path equations correspond to a rigorous quantum/classical limit within the TDSCF approximation for the total wave function. Quantum and classical degrees of freedom are coupled self-consistently through the time-dependent operator $\hat{H}_{SB}[R(t)]$ and the "quantum force" $F_R^{\text{qu}} = -\nabla_R \langle \hat{H}_{SB} \rangle_S$, respectively, i.e., they can exchange energy. If a diabatic basis, i.e., isolated solute energy eigenfunctions, or some fixed discrete variable representation (DVR) grid in position space is used for a representation of the state vector $|\varphi_S\rangle$, the expression for the quantum force simplifies to

$$F_R^{\text{qu}} \equiv -\nabla_R \langle \hat{H}_{SB} \rangle_S = -\langle \nabla_R \hat{H}_{SB} \rangle_S \equiv F_R^{\text{HF}}. \tag{18}$$

Equation (18) is of the general form of a Hellmann-Feynman theorem [29,30].

Various integration schemes for QCMD simulations have been described, see, e.g., Ref. [31]. We have chosen to use the PICKAPACK algorithm developed by Schütte and coworkers [32,33]. It has the important property of being symplectic and symmetric. When studying energy transfer by molecular dynamics simulation, the conservation of total energy and momentum is absolutely essential. Regarding the symplectic property, we mention that the conservation of total energy and momentum in mean field QCMD is only defined on the level of expectation values, but obviously does

not hold on a quantum state-to-state level. This will become important later on. The PICKAPACK propagator consists in the following subsequent steps:

$$R_{0.5}=R_0+\frac{p_{R,0}}{M}\frac{\Delta t}{2},$$

$$|\varphi_S\rangle_{0.5}=\exp\left\{-\frac{i}{\hbar}\hat{K}_q\frac{\Delta t}{2}\right\}|\varphi_S\rangle_0; \tag{19a}$$

$$p_{R,1}=p_{R,0}-\{\langle\nabla_R\hat{V}_q(r,R_{0.5})\rangle_{0.5}+\nabla_R H_B(R_{0.5})\}\Delta t,$$

$$|\varphi_S\rangle_1=\exp\left\{-\frac{i}{\hbar}\hat{K}_q\frac{\Delta t}{2}\right\}\exp\left\{-\frac{i}{\hbar}\hat{V}_q(r,R_{0.5})\Delta t\right\}|\varphi_S\rangle_{0.5}; \tag{19b}$$

$$R_1=R_{0.5}+\frac{p_{R,1}}{M}\frac{\Delta t}{2}, \tag{19c}$$

where subscripts 0, 0.5, and 1 denote dynamical variables and wave functions at times t, $t+\Delta t/2$, and $t+\Delta t$, respectively. $\hat{K}_q$ is the kinetic energy operator of the quantum vibrational degree of freedom, and $\hat{V}_q(r,R(t))\equiv U_S(r)+V(r,R(t))=\hat{U}_S+\hat{H}_{SB}[R(t)]$ is the sum of solute internal and solute-solvent potential energy operators according to Eq. (13).

Usually, one would switch back and forth between the position and momentum representation of the quantum state vector in order to evaluate the split operator kinetic and potential propagators exactly. Since, however, the momentum representation is of no value to us other than just for doing the kinetic propagation, we use a modified scheme [31], where the symmetric splitting of the quantum propagator is done according to

$$|\varphi_S\rangle_1=\exp\left\{-\frac{i}{\hbar}\hat{H}_S\frac{\Delta t}{2}\right\}\exp\left\{-\frac{i}{\hbar}\hat{H}_{SB}[R_{0.5}]\Delta t\right\}\times\exp\left\{-\frac{i}{\hbar}\hat{H}_S\frac{\Delta t}{2}\right\}|\varphi_S\rangle_0.$$

Now the position and $\hat{H}_S$ eigenfunction (diabatic basis) representations can be employed to integrate the mean field Ehrenfest equations of motion. This modified PICKAPACK scheme is also symplectic and symmetric. Although the intermediate state vector $|\varphi_S\rangle_{0.5}$ is different from the original formulation, the results obtained are not changed.

Besides the time-dependent expectation values of the various energy terms along a simulated trajectory, the analytic computation of the time derivative of energies (power) and the work terms obtained therefrom by numerical integration, have proven a valuable tool for the mechanistic analysis of energy flow in nonequilibrium simulations of energy transfer processes [21,22]. In a fully classical mechanical treatment, the time derivative of the energy (power, capacity) corresponding to linear types of motion, e.g., translational or vibrational, is given by [34]

$$N_r(t)\equiv\frac{dE_r}{dt}=F_r^e\cdot v_r,\quad F_r^e=-\nabla_r V(r,R). \tag{20}$$

Equation (20) is written with the system/bath partitioning of Eq. (13) in mind, where r and R denote the positions of the system and the bath DOF, respectively. From the time-dependent capacity (power) $N_r(t)$ the external work done by the environmental degrees of freedom upon the system can easily be obtained by numerical integration,

$$W_r^e(t)=\int_0^t N_r(\tau)d\tau. \tag{21}$$

The analytical concept of time-dependent capacity is straightforwardly extended to the quantum or quantum/classical domain by using the time dependence of an expectation value $\langle\hat{\Omega}\rangle$ [35],

$$\frac{d\langle\hat{\Omega}\rangle}{dt}=\frac{i}{\hbar}\langle[\hat{H},\hat{\Omega}]\rangle+\left\langle\frac{\partial\hat{\Omega}(t)}{\partial t}\right\rangle, \tag{22}$$

where the second term on the right hand side takes account of a possible time dependence in the Schrödinger representation. In quantum molecular dynamics capacities are time derivatives of the expectation values of Hamiltonian operators. Hence, the relevant capacities for our model quantum/classical Hamiltonian are as follows:

$$\frac{d\langle\hat{H}_S\rangle}{dt}=\frac{i}{\hbar}\langle[\hat{H}_q(t),\hat{H}_S]\rangle=\frac{i}{\hbar}\langle[\hat{H}_{SB}[R(t)],\hat{H}_S]\rangle, \tag{23}$$

$$\frac{d\langle\hat{H}_q(t)\rangle}{dt}=\left\langle\frac{\partial\hat{H}_{SB}[R(t)]}{\partial t}\right\rangle=\left\langle\frac{\partial\hat{H}_{SB}[R(t)]}{\partial R}\right\rangle\dot{R}(t), \tag{24}$$

$$\frac{d\langle\hat{H}_{SB}[R(t)]\rangle}{dt}=-\frac{d\langle\hat{H}_S\rangle}{dt}+\frac{d\langle\hat{H}_q(t)\rangle}{dt}, \tag{25}$$

$$\frac{dH_B}{dt}=-\left\langle\frac{\partial\hat{H}_{SB}[R(t)]}{\partial R}\right\rangle v_R(t)=-\left\langle\frac{d\hat{H}_q(t)}{dt}\right\rangle. \tag{26}$$

In Eqs. (24) and (26) the validity of the Hellmann-Feynman force has been assumed. Numerical integration of these analytical expressions gives a corresponding work term according to Eq. (21). The sum of Eqs. (23), (25), and (26), or equivalently the sum of Eqs. (24) and (26), must be equal to zero, which can be used to check the conservation of total energy.

III. MODEL AND SIMULATION PROCEDURE

In the present work we employ the simple model Hamiltonian of a harmonic breathing sphere embedded in a Lennard-Jones fluid at a reduced solvent density $\varrho^*\equiv\varrho_N\sigma^3=0.75$ to test the performance of the mean field quantum/classical approximation against fully classical simulations for vibrational energy relaxation in solution. For a solvent Lennard-Jones diameter of $\sigma_{\mathrm{solv}}=3.405$ Å, as used

in the parametrization specified below, the solvent number density is $\varrho_N \simeq 0.019$ Å^{-3}.

The precise form of our model Hamiltonian is as follows. The system, i.e., isolated breathing sphere, Hamiltonian $\hat{H}_S$ is

$$\hat{H}_S = -\frac{\hbar^2}{2\mu}\frac{\partial^2}{\partial r^2} + \frac{k_{\text{force}}}{2}(\Delta r)^2, \tag{27}$$

where μ is the reduced mass of the quantum vibrational degree of freedom, and $k_{\text{force}} = \mu\omega_0^2$ is the harmonic breathing sphere force constant given in terms of the reduced mass and vibrational angular frequency ω_0. The meaning of the vibrational displacement variable Δr will become more transparent below. The solvent bath Hamiltonian H_B is the sum of kinetic energies K_i and interaction energies U_{ij} of solvent particles with positions and momenta $\{(\vec{R}_i, \vec{p}_{R,i})\}$,

$$H_{\text{bath}} = \sum_i K_i + \sum_{i<j} U_{ij}, \tag{28}$$

where the solute (breathing sphere) center of mass $(\vec{R}_c, \vec{p}_c)$ kinetic energy

$$K_c = \frac{m_c}{2}|\vec{v}_c|^2 = \frac{|\vec{p}_c|^2}{2m_c}$$

is included in the sum $\Sigma_i K_i$. Formally, the reduced mass μ and the solute total mass m_c may be related to the masses m_1 and m_2 of an effective diatomic solute through

$$m_c = m_1 + m_2, \quad \mu = \frac{m_1 m_2}{m_c}.$$

The specific functional form of solvent-solvent potential energies U_{ij} is assumed to be of Lennard-Jones 12-6 type,

$$U_{ij}(R_{ij}) = 4\epsilon_{\text{solv}}\left\{\left(\frac{\sigma_{\text{solv}}}{R_{ij}}\right)^{12} - \left(\frac{\sigma_{\text{solv}}}{R_{ij}}\right)^{6}\right\}, \quad R_{ij} = |\vec{R}_i - \vec{R}_j|. \tag{29}$$

For the solute-solvent interaction energy, which is equal to the system-bath Hamiltonian $\hat{H}_{SB}$ in our terminology, we have chosen a sum of modified Kihara potentials,

$$\langle r|\hat{H}_{SB}|r\rangle = \sum_j U_{cj}(\Delta r, R_{cj}) = \sum_j 4\epsilon_S\left\{\left(\frac{\sigma_S}{R_{cj} - \alpha\Delta r}\right)^{12} - \left(\frac{\sigma_S}{R_{cj} - \alpha\Delta r}\right)^{6}\right\}, \tag{30}$$

where $\alpha = 0.5$. We note here that our breathing sphere Hamiltonian differs from the one which is frequently used to model VER in solution, e.g., Ref. [36]. While the latter model employs a harmonically breathing solute-solvent Lennard-Jones diameter $\sigma_S = \sigma_0 + \alpha\Delta r$, we identify the vibrational breathing sphere coordinate as a fluctuating hard sphere diameter, which shifts the interaction energy and force between the solute center of mass and the ith solvent atom along the distance axis, but does not change the shape of these functions.

According to the PICKAPACK algorithm described in Eq. (19), the system-bath interaction Hamiltonian $\hat{H}_{SB}[R(t)] = H_{SB}[r, R(t)]$ as well as the forces experienced by the classical degrees of freedom, i.e., $\vec{F}_c(t)$ and $\vec{F}_i(t)$, have to be evaluated at intermediate times $t + \Delta t/2$. From Eqs. (29) and (30) we get

$$\vec{F}_c \equiv -\sum_j \left\langle \frac{\partial U_{cj}[\Delta r, R_{cj}(t+\Delta t/2)]}{\partial R_{cj}} \right\rangle_{t+\Delta t/2} \frac{\vec{R}_{cj}}{R_{cj}} = \sum_j \vec{F}_{cj},$$

$$\vec{F}_i \equiv -\vec{F}_{ci} - \sum_j \frac{\partial U_{ij}[R_{ij}(t+\Delta t/2)]}{\partial R_{ij}} \frac{\vec{R}_{ij}}{R_{ij}} = \vec{F}_{ic} + \sum_j \vec{F}_{ij}. \tag{31}$$

The capacity (power) exerted upon the time-dependent quantum Hamiltonian $\hat{H}_q(t) = \hat{H}_S + \hat{H}_{SB}[R(t)]$, as calculated from Eqs. (24) and (26),

$$\frac{d\langle \hat{H}_q(t)\rangle}{dt} = -\frac{dH_B}{dt} = -\sum_j \vec{F}_{cj}\cdot\vec{v}_{cj}, \quad \vec{v}_{cj} = \vec{v}_c - \vec{v}_j, \tag{32}$$

is determined by the quantum-averaged forces $\vec{F}_{cj}$ upon the solute center of mass, since all effects of bath internal forces $\vec{F}_{ij}$ cancel out.

The time step Δt used to solve the coupled quantum/classical equations of motion may generally be set equal to $\Delta t \simeq 0.01 \times 2\pi/\omega(n_{\max})$, where $\omega(n_{\max}) = \omega_0\{n_{\max} + 1/2\}$ is the angular frequency corresponding to the quantum amplitude of the highest eigenstate of $\hat{H}_S$ included in the time evolved state vector,

$$\exp\left\{-\frac{i}{\hbar}\hat{H}_S\frac{\Delta t}{2}\right\}|\varphi_S\rangle = \sum_{n=0}^{n_{\max}} \exp\left\{-\frac{i\omega_n\Delta t}{2}\right\}|n\rangle\langle n|\varphi_S\rangle.$$

In our simulations starting from a mean quantum number of $\langle\hat{n}\rangle = 5$, we set $n_{\max} = 20$ to ensure that the amplitudes of coherent wave packets (see below) remain sufficiently small for $n = n_{\max}$, resulting in $\Delta t \simeq 0.1$ fs. In practice, Δt values up to ten times as large may be used without loss of accuracy, because the main effect of the solvent environment is to shift the vibrational potential energy function vertically (solvation), while fluctuating changes in the shape of this function are small.

The parametrization of our model Hamiltonian has been chosen to meet the conditions used to model ground state I_2 in argon clusters [37]. Parameters μ, ω_0, m_c, ϵ_S, σ_S, m_{solv}, ϵ_{solv}, σ_{solv} are summarized in Table I. Simulations have been performed within the *NVE* ensemble (constant particle number, volume, and total energy) at average temperature $T = 300$ K, resulting in a reduced temperature of $T^* \equiv k_B T/\epsilon_{\text{solv}} = 2.503$. Thus, the thermodynamic conditions specified by ϱ^* and T^* correspond to a supercritical liquidlike state ($T^* > T_c^* \simeq 1.316, \varrho^* > \varrho_c^* \simeq 0.304$) [38]. The inevitable rise of solvent temperature during nonequilibrium

TABLE I. Mass and interaction parameters for our model breathing sphere in a Lennard-Jones fluid.

μ (amu)	ω_0 (cm^{-1})	m_c (amu)	ϵ_S (cm^{-1})	σ_S (Å)	m_{solv} (amu)	ϵ_{solv} (cm^{-1})	σ_{solv} (Å)
63.45	220	253.8	130.3	3.617	39.95	83.3	3.405

energy redistribution in a microcanonical ensemble can be kept within an acceptable range by appropriately adjusting the total heat capacity (system size). In our case a value of $N_{solv}=500$ for the number of solvent atoms is enough to achieve $\Delta T<5$ K.

In order to generate an ensemble of initial conditions for the classical degrees of freedom, we start from a breathing sphere constrained to $\Delta r=0$, centered in a cubic box and embedded in a fcc lattice of solvent particles. This configuration is equilibrated for 100 ps by repeatedly rescaling velocities to the desired target temperature of 300 K. Additional classical initial conditions are picked up after subsequent periods of 10 ps length.

For each set of classical initial positions and momenta of bath particles the breathing sphere is prepared with an expectation value of five vibrational quanta, where the wave function corresponds either to a (diabatic) eigenstate $|n\rangle$ of $\hat{H}_S$, to a coherent state specified by [39]

$$|\alpha\rangle=\exp\left\{-\frac{|\alpha|^2}{2}\right\}\sum_{n=0}^{n_{\max}}\frac{\alpha^n}{\sqrt{n!}}|n\rangle \tag{33}$$

in terms of harmonic oscillator (HO) basis functions, or to a superposition state intermediate between $|\alpha\rangle$ and $|n\rangle$. Coherent states are eigenstates of the annihilation operator $\hat{a}$, i.e., $\hat{a}|\alpha\rangle=\alpha|\alpha\rangle$ and $\langle\alpha|\hat{a}^+=\langle\alpha|\alpha^*$, where the coherent state parameter α determines the initial vibrational phase of the corresponding HO through

$$\langle\Delta r\rangle_\alpha=\sqrt{\frac{\hbar}{2\mu\omega_0}}\{\alpha+\alpha^*\}$$

and

$$\langle p_r\rangle_\alpha=-i\sqrt{\frac{\mu\hbar\omega_0}{2}}\{\alpha-\alpha^*\},$$

and the mean occupation number is given by $\langle\hat{n}\rangle_\alpha \equiv\langle\alpha|\hat{a}^+\hat{a}|\alpha\rangle=|\alpha|^2$. The uncertainties in position and momentum space associated with these wave packets are minimal as measured by the product of standard deviations, $\sigma_r\times\sigma_{p_r}=\hbar/2$, and thus coherent states are the most classical-like wave packets that may be constructed.

Ensemble averaging over 50–100 trajectories is typically sufficient to average out statistical fluctuations. Here we employ an ensemble size of 50 individual quantum/classical time evolutions.

Potential energies and forces are computed for all interatomic distances below a cutoff R_{cut} equal to four times the largest Lennard-Jones diameter, which is σ_S in our case. Although interaction energies and forces at such R_{cut} values are vanishingly small, artificial high frequency components in the spectral density of forces can principally arise from the motion of atoms across the cutoff region. Therefore, we choose to (vertically) shift and smooth potentials $U(R)$ according to

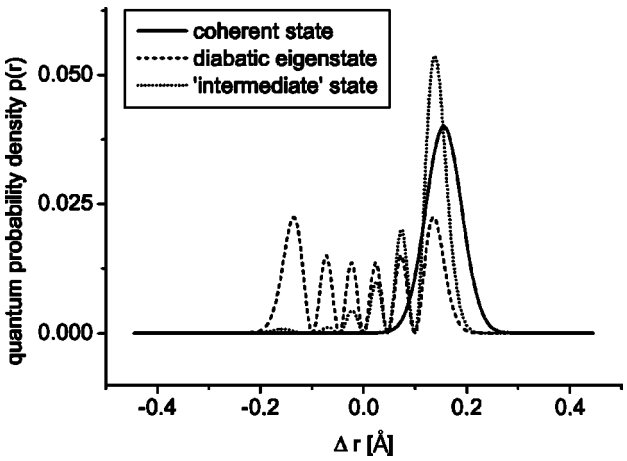

FIG. 1. Quantum probability density in position space associated with the three types of quantum initial states at given mean vibrational energy employed in quantum/classical simulations.

$$U(R)=U_{LJ}(R)-U_{LJ}(R_{cut})-\left\{\frac{\partial U_{LJ}(R)}{\partial R}\right\}_{R=R_{cut}}(R-R_{cut}), \tag{34}$$

where $U_{LJ}(R)$ is the original Lennard-Jones interatomic potential. The resultant forces are thus given by

$$F_R(R)\equiv-\nabla_R U(R)=-\nabla_R U_{LJ}(R)+\{\nabla_R U_{LJ}(R)\}_{R=R_{cut}}. \tag{35}$$

The modified potentials and forces satisfy $U(R_{cut})=0$ and $F_R(R_{cut})=0$, respectively.

IV. RESULTS AND DISCUSSION

Among the various possible quantum initial state vectors at a given mean vibrational energy, coherent states and eigenstates of the harmonic oscillator represent wave functions of extremely different character. While coherent states are the most classical-like quantum states that may be constructed, eigenfunctions of the HO Hamiltonian do not possess a classical analog and a classical vibrational phase can therefore not be assigned. Figure 1 illustrates the three types of initial state vectors, namely, coherent, diabatic, and ''intermediate'' wave packet, in the position space representation.

Before we give a detailed account of the results obtained from quantum/classical simulations of vibrational energy relaxation for the various quantum initial conditions, we briefly mention that completely classical simulations using the same model Hamiltonian and parameter conditions give strictly exponential energy relaxation with a nonequilibrium relaxation time $\tau_{cl}\cong 12$ ps, which is in accord with the result of a

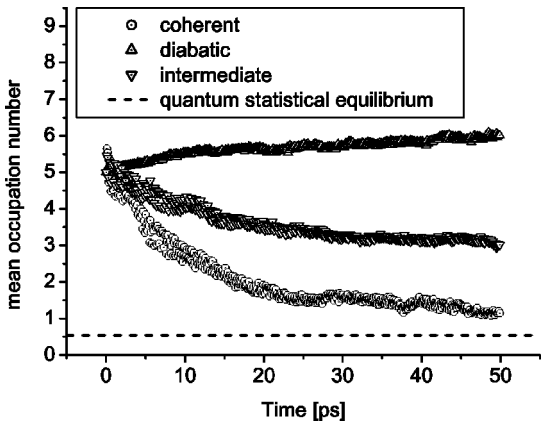

FIG. 2. Quantum/classical ensemble averaged time evolution of mean vibrational energy (in terms of mean occupation number) for different quantum initial conditions.

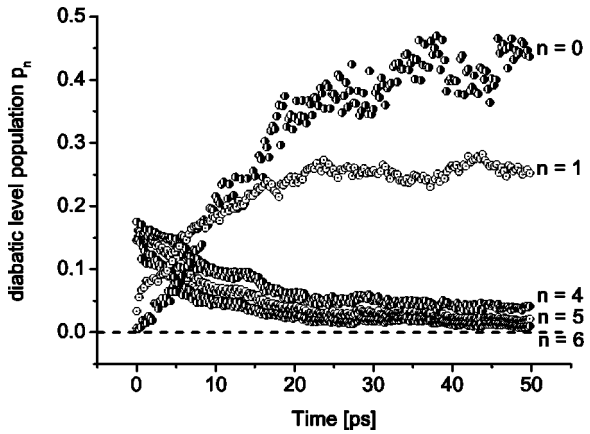

FIG. 3. Diabatic state, i.e., harmonic oscillator eigenstate, populations averaged over classical bath initial conditions for coherent initial state.

linear response treatment using the fluctuating external solvent force correlation function.

A. Mean energy relaxation

In Fig. 2 we compare the ensemble averaged mean vibrational energy—in terms of the mean occupation number $\langle \hat{n} \rangle_{S,B}$—as a function of time, starting from the different quantum initial states. Distinctly different behaviors are observed: While coherent states relax towards thermal equilibrium, the nature of which will be examined later, eigenstates experience an unphysical heating effect. We note here that this heating effect is not only an ensemble averaged property, rather it is observed also for individual quantum/classical trajectories starting from an initial eigenstate, where the mean energy is never allowed to fall below its initial value. In addition, the coherent state relaxation is—apparently—nonexponential in time. Table II reports the decay parameters obtained from a biexponential fit of the coherent state energy decay, where $\langle \hat{n} \rangle \rightarrow \overline{n}(\omega_0, T)$ is assumed as the long time limit and $\overline{n}(\omega_0, T)$ is the quantum statistical mean thermal occupation number. We will see, however, that the apparent nonexponentiality of coherent state energy relaxation is due to a misinterpretation, since the quantum statistical mean thermal occupation number at given bath temperature is not the correct stationary value at long times subject to the mean field Ehrenfest equations of motion (quantum/classical equilibrium).

Contrary to the coherent state case, an ensemble of ''intermediate'' initial superposition states does not relax towards a physically reasonable equilibrium, although energy dissipation is observed—in contrast to an ensemble of initial eigenstates. The effective vibrational temperature calculated from $\langle \hat{n} \rangle_{t \rightarrow \infty}$ at long times and the quantum statistical expression for $\overline{n}(\omega_0, T)$ is $T_{\mathrm{eff}}^{\mathrm{qu}} \simeq 1090$ K. The relaxation towards that long time limit, however, is—to a very good approximation—exponential in time (Table II), and the relaxation time obtained is larger than but close to the classical (and quantum) relaxation time.

TABLE II. Preliminary analysis of coherent and intermediate initial state energy relaxation ($\langle \hat{n} \rangle_{\alpha} \rightarrow$quantum statistical equilibrium).

Fit	τ_1 (ps)	τ_2 (ps)	$\langle \tau \rangle$ (ps)
Coherent	7.5 ± 0.4 (69%)	49 ± 1 (31%)	21
Intermediate	13.7 ± 0.3		13.7

B. Diabatic level populations

In Figs. 3 and 4, we show the decay of diabatic level populations, i.e., the diagonal elements of the density matrix in the basis of HO eigenstates, for the ensembles of coherent (Fig. 3) vs diabatic initial states (Fig. 4) with an expectation value of $\langle \hat{n} \rangle = 5$ at time zero. The analysis reveals that the quantum/classical ensemble of coherent initial states relaxes towards a quasicanonical distribution at long times (see below), while the ensemble of diabatic initial states does not.

For the latter initial conditions it is clearly visible that, while the initially occupied level ($n=5$) is depopulated, the levels $n = 5 \pm 1$ are populated with essentially the same probability at a given time. The same is true for $n = 5 \pm 2$ (not shown) and almost true for $n = 5 \pm 3$. Thus, the stochastic evolution of diabatic level populations in the diabatic initial

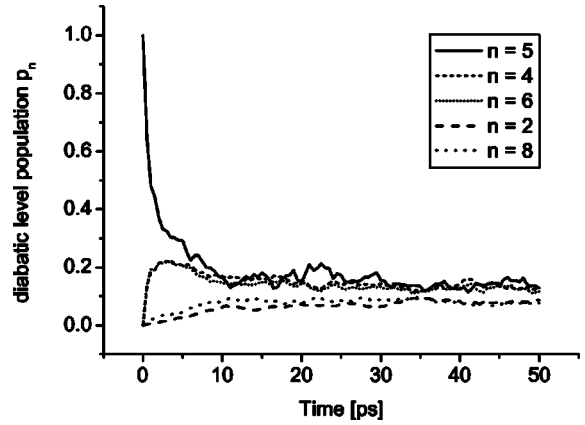

FIG. 4. The same as Fig. 3, but for diabatic initial state.

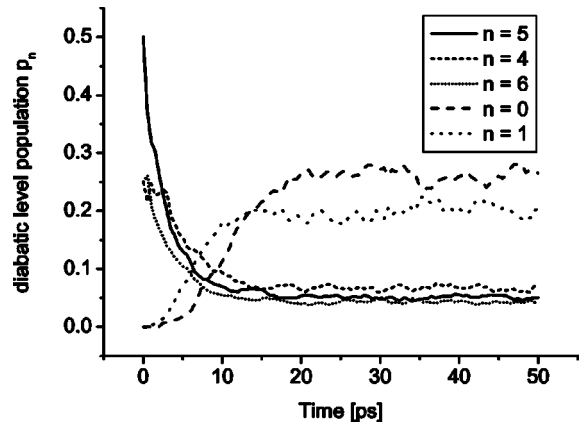

FIG. 5. The same as Fig. 3, but for intermediate initial superposition state.

state case corresponds to (unbiased) ''diffusion'' in energy space at early times, affected by the lower bound ($n=0$) of the Hilbert space of diabatic basis functions at later times, which naturally explains the heating effect. A more detailed analysis will be given below.

In Fig. 5 is shown the evolution of diabatic level populations for an ensemble of intermediate initial superposition states, which—as in the coherent case—relaxes towards a quasicanonical distribution.

Figure 6 summarizes the results obtained for the various quantum initial conditions by comparing the final level populations at $t=50$ ps: Relaxation towards quasicanonical distributions for initial superposition states (coherent and intermediate) with effective vibrational temperatures of $T_{\mathrm{eff}}^{\mathrm{qu}}\simeq 490$ and $T_{\mathrm{eff}}^{\mathrm{qu}}\simeq 1115$ K at $t=50$ ps, respectively; diffusion in energy space for a diabatic initial state. Thus, in the latter case, a *breakdown of detailed balance* clearly emerges as a consequence of the mean field Ehrenfest quantum/classical equations of motion. The same applies, to some extent, also to the intermediate-type initial superposition state. This will become more clear, when we analyze the nature of quantum/classical equilibrium.

Considering the basic ingredients of the mean field Ehrenfest equations of motion (EOM), our results described so far

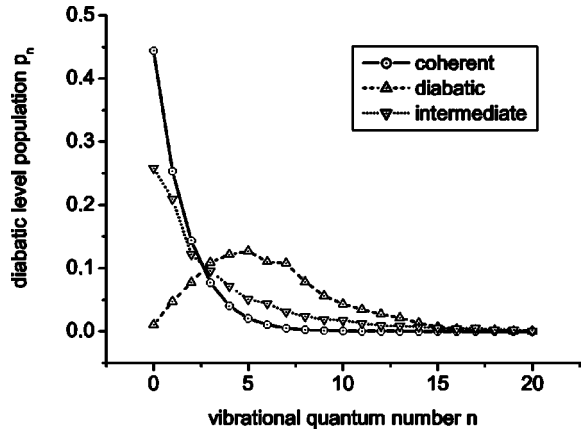

FIG. 6. Diabatic level populations at $t=50$ ps for different quantum initial conditions.

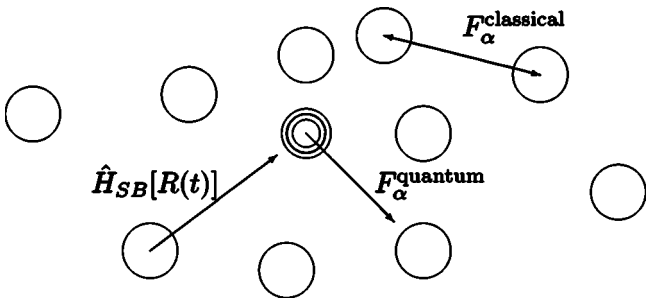

FIG. 7. Illustration of interactions between quantum and classical degrees of freedom in our model system according to the mean field Ehrenfest ansatz.

may be explained as follows. Molecular friction is a correlation effect, i.e., it emerges from a backreaction of the bath degrees of freedom upon the motion of the relevant system DOF, where—under the quantum/classical EOM—the classical environmental DOF monitor the motion and energy content of the quantum system only via an expectation value, i.e., a Hellmann-Feynman-type force. This is schematically illustrated in Fig. 7. As a result, energy dissipation can within a mean-field-type quantum/classical approach only arise, if the mean energy content of the quantum subsystem reveals itself at least to some extent through a dynamic evolution of expectation values associated with the quantum system under the action of the bare system Hamiltonian $\hat{H}_S$. While this is true for superposition states constructed from eigenstates of $\hat{H}_S$, it is definitely not for the eigenstates themselves. More specifically, for a coherent state, i.e., a minimum uncertainty wave packet, the expectation value of energy is completely defined through the expectation values of position and momentum which move in time as in classical mechanics. For an eigenstate of $\hat{H}_S$, however, the energy is exclusively encoded in the shape of the wave function, i.e., its nodal structure, which has little effect on the Hellmann-Feynman force. Arbitrary (intermediate) superposition states are located inbetween the two limiting cases, i.e., part of the mean energy is encoded in terms of nonstationary expectation values and part of it is encoded in the nodal structure of the wave function (see Fig. 1).

C. Heisenberg uncertainty relation

Since the way, how the mean energy $\langle \hat{H}_S \rangle$ is encrypted in the shape of the system wave function, is tied to the delocalization in position space, we might expect that the dynamic evolution of mean energy relaxation, i.e., the energy relaxation time(s), is affected by the uncertainty in position (and momentum) space at time zero as well as its dynamic evolution averaged over the quantum/classical ensemble. A natural starting point for investigating this perspective is the Heisenberg uncertainty relation,

$$\sigma_{\Delta r}\sigma_p \geqslant \frac{\hbar}{2}, \tag{36}$$

where the equality sign holds for coherent (minimum uncertainty) wave packets. Figure 8 shows the quantum/classical

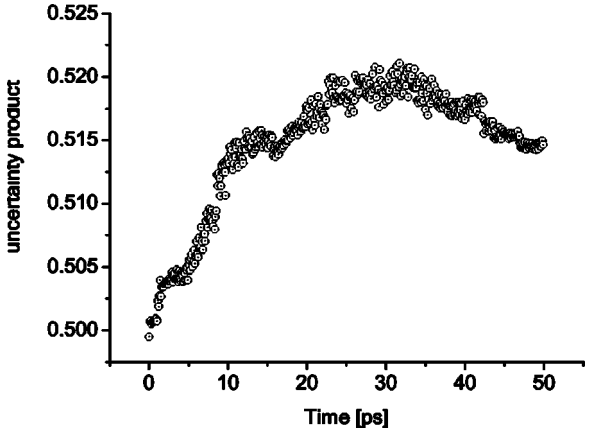

FIG. 8. Quantum/classical ensemble averaged time evolution of position-momentum uncertainty product (in units of $\hbar$) for coherent initial state.

ensemble averaged evolution of $\sigma_{\Delta r}\sigma_p$ as a function of time for the coherent initial state case. An increase of the uncertainty product is observed which amounts to $\approx$4% occurring on a time scale of $\tau \simeq 10$ ps, which is on the order of the classical energy relaxation time $\tau_{\rm cl} \cong 12$ ps.

For an eigenstate of the HO Hamiltonian with quantum number n the uncertainty product is equal to $\sigma_{\Delta r}\sigma_p = \hbar\ (n+\frac{1}{2})$. Here, an increase is also observed (not shown), which is, however, below 1%. As Fig. 6 implies, the increase of the uncertainty product is due to the population of higher excited vibrational states. Thus, ensembles of coherent or diabatic quantum initial states are relatively stable with respect to a relative increase of the uncertainty product.

Figure 9 shows the ensemble averaged evolution of $\sigma_{\Delta r}\sigma_p$ for the intermediate initial state case. Here, the uncertainty product amounts to $\sigma_{\Delta r}\sigma_p \simeq 2.4\ \hbar$ at $t=0$ and a relative increase of $\approx$23% is observed on a time scale of $\tau \simeq 10$ ps, while at later times $\sigma_{\Delta r}\sigma_p$ decreases again, as observed for an ensemble of coherent initial states (Fig. 8).

If we would assume that the dynamic growth of uncertainty in position space will affect the time scale of energy relaxation subject to the mean field quantum/classical EOM then we would be forced to expect nonexponential energy relaxation for the ensemble of intermediate superposition states, which is, however, not observed. Considering the coherent initial state case, we are led to the conclusion that the—artifactual—nonexponential relaxation cannot be due to the observed small dynamic increase of $\sigma_{\Delta r}\sigma_p$.

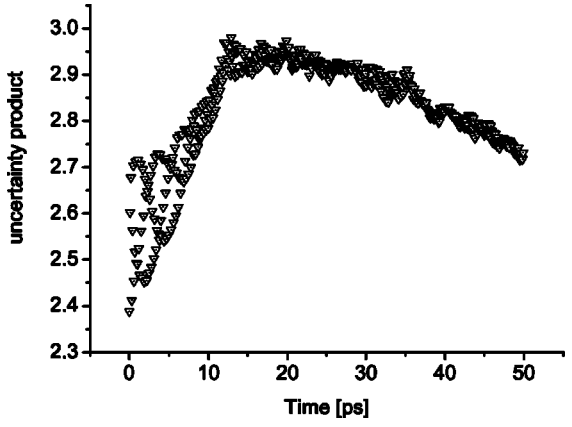

FIG. 9. The same as Fig. 8, but for intermediate initial state.

D. Breakdown of detailed balance

To theoretically investigate the approach towards quantum/classical equilibrium, it is convenient to start with a Pauli quantum master equation (QME) [39],

$$\frac{dp_n}{dt} = -\left\{\sum_m k_{n\to m}\right\} p_n + \sum_m k_{m\to n} p_m , \qquad (37)$$

for the (diabatic) level populations p_n, where the state-to-state rate coefficients $k_{m\to n}$ have to satisfy the detailed balance constraint

$$\frac{k_{n\to m}}{k_{m\to n}} = \left(\frac{p_m}{p_n}\right)_{\rm eq} \equiv \exp\left\{-\frac{\Delta E_{mn}}{k_B T_{\rm bath}}\right\},$$

in order to drive an arbitrary initial population of energy levels towards the correct thermal equilibrium distribution defined by the bath temperature.

A complete neglect of detailed balance, as apparently observed in Sec. IV B at early times for the diabatic level populations starting from an ensemble of diabatic initial states (''diffusion'' in energy space), would ultimately lead to a uniform distribution among the energy states characterized by an effective temperature of $T_{\rm eff}\to\infty$. To investigate whether this is the asymptotic limit for diabatic initial states subject to the mean field quantum/classical EOM, and to establish a connection between the quantum state-to-state rates and the classical rate of energy relaxation, we use the golden rule [35,40] assuming that the dissipative effect of the system-bath interaction can be treated by the first-order perturbation theory.

According to the golden rule expression in the time domain,

$$k_{m\to n} = \frac{1}{\hbar^2}\int_{-\infty}^{+\infty} dt e^{i\omega_{mn}t}\langle \hat{V}_{mn}(t)\hat{V}_{nm}(0)\rangle_{qB}, \qquad (38)$$

the state-to-state rate coefficient is proportional to the Fourier transform of a quantum-bath correlation function, evaluated at the transition frequency $\omega_{mn}=\omega_m-\omega_n$. The term $\hat{V}_{mn}(t)$ is a matrix element in the (diabatic) system basis $\{|n\rangle\}$ of the system-bath interaction $\hat{H}_{SB}=\hat{V}_{\rm int}$ in the interaction picture. Since $\langle \hat{V}_{mn}(t)\hat{V}_{nm}(0)\rangle_{qB}$ is a complex-valued function of time, it cannot be directly substituted by the classical real-valued function $\langle V_{mn}(t)V_{nm}(0)\rangle_{\rm cl}$. Direct replacement of $\langle \hat{V}_{mn}(t)\hat{V}_{nm}(0)\rangle_{qB}$ by the classical correlation function leads to neglect of detailed balance from the start. As described by Oxtoby and by Okazaki [41,23], one way to circumvent this problem while using the classical correlation function is to employ the detailed balance relationship between $k_{m\to n}$ and $k_{n\to m}$, and to exploit the properties of quantum mechanical correlation functions [40], yielding

$$k_{m\to n}=\frac{1}{\hbar^2}\frac{2}{1+e^{-\beta\hbar\omega_{mn}}}\int_{-\infty}^{+\infty}dt e^{i\omega_{mn}t}\times\langle\tfrac{1}{2}[\hat{V}_{mn}(t),\hat{V}_{nm}(0)]_+\rangle_{qB}, \tag{39}$$

where the symmetrized quantum correlation function may be replaced by its classical analog $\langle V_{mn}(t)V_{nm}(0)\rangle_{\rm cl}$. The prefactor in Eq. (39) contains the detailed balance constraint $e^{-\beta\hbar\omega_{mn}}=k_{n\to m}/k_{m\to n}$, where $\beta=1/k_BT$. By assuming that $\hat{V}_{\rm int}$ is linear or almost linear in the oscillator displacement $\Delta\hat{r}$, i.e., $V_{mn}(t)\simeq -F_r^e(t)\Delta r_{mn}$, we arrive at the expression

$$k_{m\to n}\simeq\frac{1}{\hbar^2}\frac{2|\Delta r_{mn}|^2}{1+e^{-\beta\hbar\omega_{mn}}}\int_{-\infty}^{+\infty}dt e^{i\omega_{mn}t}\langle F_r^e(t)F_r^e(0)\rangle_{\rm cl} \tag{40}$$

for the state-to-state rate coefficients in terms of a fluctuating external force correlation function $\langle F_r^e(t)F_r^e(0)\rangle_{\rm cl}$. If and only if we employ the linearity ansatz for $\hat{H}_{SB}=\hat{V}_{\rm int}$ can we establish a connection between $k_{m\to n}$ and the classical frequency-dependent friction coefficient. The matrix elements Δr_{mn} allow for single-quantum transitions only, and the rate constants starting from level n can be brought into the simple form

$$k_{n\to n+1}=\overline{K}\overline{n}(n+1)=k_{0\to 1}(n+1), \tag{41}$$

$$k_{n\to n-1}=\overline{K}(\overline{n}+1)n=k_{1\to 0}n, \tag{42}$$

where $\overline{K}$ is the average rate of energy relaxation and $\overline{n}$ denotes the mean thermal occupation number. Detailed balance is incorporated through

$$\frac{k_{n\to n+1}}{k_{n+1\to n}}\equiv\frac{k_{0\to 1}}{k_{1\to 0}}=\frac{\overline{n}}{\overline{n}+1}\equiv e^{-\beta\hbar\omega_0},\quad \overline{n}=\{e^{\beta\hbar\omega_0}-1\}^{-1}.$$

The quantum average rate constant of energy relaxation is related to the classical rate through

$$\overline{K}\equiv\overline{K}_{\rm qu}=\frac{k_BT_{\rm bath}}{\hbar\omega_0(\overline{n}+1/2)}\overline{K}_{\rm cl} \tag{43}$$

where the classical rate coefficient, which is equal to the frequency-dependent friction coefficient at $\omega=\omega_0$, is in turn related to the external force correlation function via a fluctuation-dissipation theorem [42],

$$\overline{K}_{\rm cl}\equiv\gamma(\omega_0)=\frac{1}{\mu k_BT}\int_0^\infty dt\cos(\omega_0t)\langle F_r^e(t)F_r^e(0)\rangle_{\rm cl}. \tag{44}$$

In this simplified treatment we neglect the frequency shift $\Delta\omega$ induced by the average static effect of the solvent environment. The quantum prefactor in Eq. (43) defining the ratio $\overline{K}_{\rm qu}/\overline{K}_{\rm cl}$ is nothing but the ratio of the classical mean thermal energy of a vibrational DOF vs the quantum statistical mean energy of the same oscillator at a given bath temperature. This ratio cannot become larger than unity, which is a consequence of the linearity ansatz for $\hat{H}_{SB}$ used in the derivation. If multiquantum transitions become important, i.e., the linearity ansatz breaks down, the relation implied by Eq. (43) does no longer hold. However, our results obtained from quantum/classical simulations seem to justify the linearized treatment described above. In fact, the parameter conditions of our model system were chosen such as to obtain a suitably short energy relaxation time as a result of the relatively small vibrational frequency (energy level spacing). Thus, by construction the quantum energy level spacing is located in the frequency regime where the external force spectral density is still large, and it is sufficient to keep the dominant linear term only in the expansion of $\hat{H}_{SB}$ (see the discussion in Ref. [20]).

In order to see how the neglect of detailed balance emerges, and to theoretically predict the resultant energy increase induced by the bath fluctuations, we write the linear rate equation for the expectation value of the number operator $\langle\hat{n}\rangle$, as may easily be derived from the Pauli QME, in the form

$$\frac{d\langle\hat{n}\rangle}{dt}=-(k_{1\to 0}-k_{0\to 1})\langle\hat{n}\rangle+k_{0\to 1}\equiv-\overline{K}\{\langle\hat{n}\rangle-\overline{n}(\omega_0,T)\}, \tag{45}$$

where $(k_{1\to 0}-k_{0\to 1})=\overline{K}$ and $k_{0\to 1}=\overline{K}\,\overline{n}$. Breakdown of detailed balance is equivalent to neglecting unity against $\overline{n}$, i.e., setting $k_{1\to 0}=k_{0\to 1}$. In the same sense, we have to neglect the zero point energy in the denominator of the quantum prefactor [Eq. (43)]. As a result, we arrive at the following expressions:

$$\overline{K}\equiv\frac{k_BT}{\hbar\omega_0\overline{n}}\gamma(\omega_0), \tag{46}$$

$$k_{1\to 0}=k_{0\to 1}\equiv\overline{K}\overline{n}=\frac{k_BT}{\hbar\omega_0}\gamma(\omega_0). \tag{47}$$

For later reference, we note that the precise relation of $\overline{n}$ to frequency and temperature is unimportant for the determination of $k_{0\to 1}$, because $\overline{n}$ cancels by Eqs. (46) and (47). From Eqs. (45)–(47) we see, that neglecting detailed balance leads to a linear increase of energy of the quantum vibrational degree of freedom, the slope being equal to $k_{0\to 1}$. In this limit, the ratio of $k_{0\to 1}$ vs the classical damping rate $\gamma(\omega_0)$ is nothing but the classical limit of the mean thermal occupation number (assuming $\beta\hbar\omega_0\ll 1$), implying that within a time $t=\tau_{\rm cl}$ the energy increases by k_BT.

In Fig. 10 we compare this prediction to the results of mean field Ehrenfest simulations starting from an ensemble of diabatic eigenstates. Instead of an *unbounded* linear energy growth, we observe a *controlled*, exponential-type increase of vibrational energy. Comparison to a Pauli QME simulation with the same number of HO basis states as used

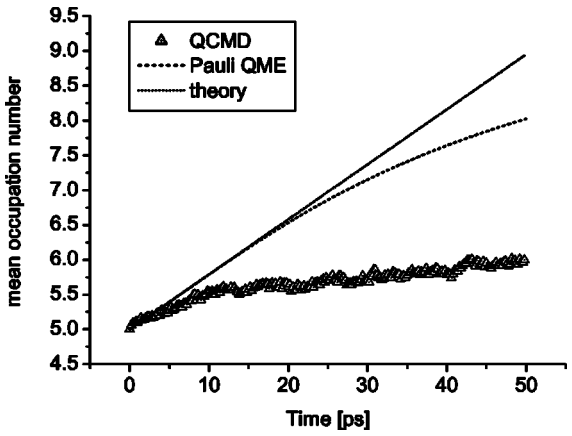

FIG. 10. Comparison of the energy growth obtained by mean field QCMD for a diabatic initial state to the results of a quantum master equation analysis assuming a complete neglect of detailed balance.

in the QCMD simulations ($n_{\max}=20$) clearly illustrates that the saturation observed via QCMD is not due to a truncation of basis, which has, of course, been taken care of in the quantum/classical treatment. Thus, the slower-than-linear-energy increase obtained by QCMD must be due to an evolving dynamic correlation between quantum and classical subsystems as a result of the quantum system being driven into a coherence by the classical bath. We will come back to this issue.

E. Quantum/classical Langevin equation

In order to provide a basis for understanding the coherent state relaxation subject to the mean field Ehrenfest equations of motion, we derive in this section a quantum/classical Langevin equation for the coherent state parameter $\alpha(t)$ defining a minimum uncertainty wave packet for the harmonic breathing sphere vibrational degree of freedom. The small relative increase of the ensemble averaged uncertainty product observed in Sec. IV C, when starting from a coherent state initial wave packet, justifies the assumption that the evolving state vector may be fixed to $|\varphi_S(t)\rangle=|\alpha(t)\rangle$. As stated by Eq. (33), a coherent state $|\alpha(t)\rangle$ of the harmonic oscillator is a special superposition state constructed from HO basis states $|n\rangle$,

$$|\alpha(t)\rangle=\exp\left\{-\frac{|\alpha|^2}{2}\right\}\sum_n \frac{\alpha^n}{\sqrt{n!}}|n\rangle, \quad \hat{a}|\alpha\rangle=\alpha|\alpha\rangle,$$

$$\langle\alpha|\hat{\alpha}^+=\langle\alpha|\alpha^*.$$

Coherent states are eigenstates of the annihilation operator $\hat{a}$, where the coherent state parameter α is the eigenvalue. The fact that $\alpha(t)=\langle\hat{a}\rangle_\alpha$ is related via

$$\alpha(t)\equiv\langle\hat{\alpha}\rangle_\alpha=\frac{1}{\sqrt{2}}\left\{\sqrt{\frac{\mu\omega_0}{\hbar}}\langle\Delta\hat{r}\rangle_\alpha+i\frac{\langle\hat{p}_r\rangle_\alpha}{\sqrt{\mu\hbar\omega_0}}\right\}, \quad (48)$$

$$|\alpha(t)|^2\equiv\langle\hat{a}^+\hat{a}\rangle_\alpha=\langle\hat{n}\rangle_\alpha \quad (49)$$

to the expectation values of position and momentum, as well as to the expectation value of the number operator, which is a measure of energy, facilitates the derivation of a quantum/classical Langevin equation (LE) for $\alpha(t)$ from the equations of motion for $\langle\Delta\hat{r}\rangle_\alpha$ and $\langle\hat{p}_r\rangle_\alpha$. From this LE, a rate equation may, in turn, be derived for $\langle\hat{n}\rangle$. According to the Ehrenfest theorem [43], the expectation values of position and momentum are governed by the classical Newtonian equations of motion,

$$\frac{d\langle\Delta\hat{r}\rangle}{dt}=\frac{\langle\hat{p}_r\rangle}{\mu},$$

$$\frac{d\langle\hat{p}_r\rangle}{dt}=-\mu\omega_0^2\langle\Delta\hat{r}\rangle+\langle\hat{F}_r^e\rangle, \quad \hat{F}_r^e=-\nabla_r\hat{H}_{SB}[R(t)]. \quad (50)$$

Equations (50), except for the classical time dependence of $\hat{F}_r^e[R(t)]$, are exact irrespective of whether a fully correlated or approximate total many-particle wave function is employed. From these equations a generalized Langevin equation (GLE) or approximate ordinary LE may be easily obtained [42],

$$\frac{d\Delta r}{dt}=\frac{p_r}{\mu},$$

$$\frac{dp_r}{dt}=-\mu\omega_0^2\Delta r-\int_0^t\gamma(\tau)p_r(t-\tau)d\tau+\delta F_r^e(t)$$

$$\simeq-\mu\omega_0^2\Delta r-\gamma(\omega_0)p_r(t)+\delta F_r^e(t), \quad (51)$$

where expectation values have been replaced by their classical analogs. The time-dependent friction kernel $\gamma(t)$ is related to the fluctuating force correlation function through

$$\gamma(t)=\frac{1}{\mu k_B T}\langle\delta F_r^e(t)\,\delta F_r^e(0)\rangle, \quad (52)$$

where we recall that $\delta F_r^e(t)$ is to be understood as a quantum expectation value, the time dependence of which is exclusively due to random fluctuations of the (classical) bath. The approximate ordinary LE form stated by Eq. (51) is facilitated when transforming from time- to frequency-dependent friction, Eq. (44), using the fact that a harmonic oscillator has associated with it a precise, energy-independent time or frequency scale, $\omega_0=2\pi/\tau_{\rm vib}$. Using Eq. (48), we arrive at the quasiclassical LE for the coherent state parameter $\alpha(t)$,

$$\frac{d\alpha}{dt}=-i\omega_0\alpha-\frac{\gamma(\omega_0)}{2}\{\alpha-\alpha^*\}+\frac{i}{\sqrt{2}}\frac{\delta F_r^e(t)}{\sqrt{\mu\hbar\omega_0}}. \quad (53)$$

Either from the latter or, more directly, from the Pauli master equation, we obtain a rate equation, Eq. (45), for the mean occupation number $\langle\hat{n}\rangle$ in the quasiclassical limit,

$$\frac{d\langle\hat{n}\rangle_\alpha}{dt}=-\overline{K}\{\langle\hat{n}\rangle_\alpha-\overline{n}_\alpha\}\rightarrow-\gamma(\omega_0)\left\{\langle\hat{n}\rangle_\alpha-\frac{k_BT}{\hbar\omega_0}\right\},$$

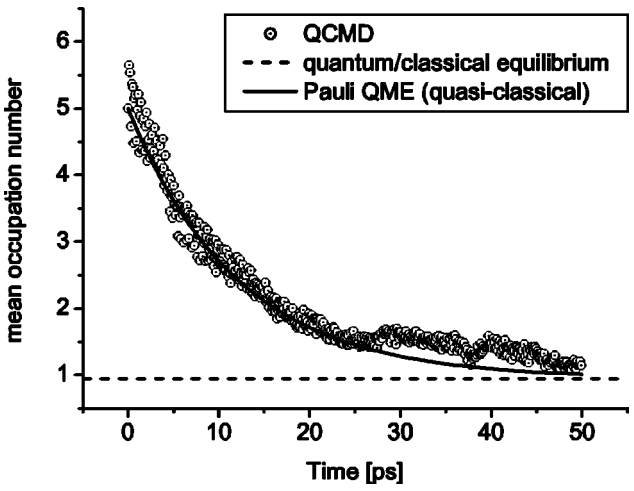

FIG. 11. Coherent initial state energy decay towards quasiclassical equilibrium (see Table III) as compared to quasiclassical Pauli QME simulation ($\tau=\tau_{\rm cl}$, $\overline{n}=k_BT/\hbar\omega_0$).

where, in the classical limit,

$$\beta\hbar\omega_0 \ll 1 \rightarrow \overline{K}=\overline{K}_{cl}, \quad \overline{n}=\frac{k_BT}{\hbar\omega_0}. \tag{54}$$

Note that Eq. (53) and also Eq. (54), when derived from Eq. (53), is exact within the mean field Ehrenfest framework, to the extent that the linear response theory holds and the wave packet is identical to a coherent state throughout the quantum/classical time evolution. The essence of this result is that an ensemble of coherent states must relax towards a quasiclassical equilibrium subject to the mean field quantum/classical EOM, irrespective of whether or not the ratio $\hbar\omega_0/k_BT$ facilitates a rigorous justification, the reason being that the bath fluctuations are described classically. For reasons of consistency with the corresponding classical fluctuation-dissipation theorem the energy relaxation time must then be equal to the classical relaxation time $\tau_{\rm cl}$.

In Fig. 11 we compare this prediction to our QCMD simulation results while fixing the long time limit of the mean occupation number to its classical value, $\langle\hat{n}\rangle_{t\rightarrow\infty} \rightarrow k_BT/\hbar\omega_0$. The result of a quasiclassical Pauli QME simulation ($\tau=\tau_{\rm cl}$, $\overline{n}=k_BT/\hbar\omega_0$) is also shown. The approach towards quasiclassical equilibrium is indeed exponential to a good approximation, the relaxation time being very close to the classical one (Table III). We honestly note here that the quantum prefactor, Eq. (43), is close to unity ($\simeq$0.917) for the model system chosen here, and therefore the quantum relaxation time is $\tau_{\rm qu}\simeq 13.1$ ps$\geqslant\tau_{\rm cl}$. So, our numerical result for coherent state relaxation is just in between the classical and the quantum relaxation time. We expect, however, that more extensive averaging over classical initial conditions will drive the numerical value more close to the classical limit. Comparison to the result of a quasiclassical Pauli QME simulation shows that the agreement is reasonably good, but statistical fluctuations have not been eliminated completely. In summary, the only quantum effect that remains, when simulating energy dissipation starting from an ensemble of coherent initial states of a HO immersed in a classical bath using the mean field Ehrenfest or classical path method, is the zero point energy constraint.

TABLE III. Fit parameters for coherent, diabatic, and intermediate initial state energy relaxation towards quantum/classical equilibrium.

Fit	τ_1 (ps)	$\langle\tau\rangle$ (ps)
Coherent	12.3 ± 0.5	12.3
Diabatic	17 ± 1	17
Intermediate	11 ± 1	11

The statistical mechanical properties of the mean field quantum/classical equations of motion emerging from the investigation of coherent state energy relaxation, lead us to a more or less straightforward interpretation of our QCMD simulation results obtained for ensembles of initial eigenstates and intermediate superposition states, respectively, by generalizing the coherent state results to arbitrary initial wave packets.

From an analysis of the quantum/classical equation of motion for the relevant system (vibrational) energy $\langle\hat{H}_S\rangle$, we can show that in the linear response regime a classical-like fluctuation-dissipation theorem holds. The time derivative of $\langle\hat{H}_S\rangle$ is given by [see Eq. (23), Sec. II]

$$\frac{d\langle\hat{H}_S\rangle}{dt}\equiv\frac{i}{\hbar}\langle[\hat{H}_q(t),\hat{H}_S]\rangle=\frac{i}{\hbar}\langle[\hat{H}_{SB}[R(t)],\hat{K}_S]\rangle$$
$$=\left\{\frac{i\hbar}{2\mu}\langle\nabla_r^2\hat{H}_{SB}[R(t)]\rangle+\langle\hat{F}_r^e[R(t)]\cdot\hat{v}_r\rangle\right\}, \tag{55}$$

where $\hat{F}_r^e[R(t)]=-\nabla_r\hat{H}_{SB}[R(t)]$ and $\hat{v}_r=\hat{p}_r/\mu$. In the linear response regime we make use of the assumption $\hat{H}_{SB}[R(t)]\simeq-\hat{F}_r^e[R(t)]\hat{r}$, and thus the external force operator $\hat{F}_r^e[R(t)]\simeq F_r^e[R(t)]$ becomes a classical function dependent on the positions of bath particles only and the second-derivative term $\nabla_r^2\hat{H}_{SB}[R(t)]$ vanishes. As a result, we end up with a classical-like expression for the $\langle\hat{H}_S\rangle$ equation of motion [see Eq. (20), Sec. II]

$$\frac{d\langle\hat{H}_S\rangle}{dt}\simeq F_r^e[R(t)]\frac{\langle\hat{p}_r\rangle}{\mu}=F_r^e[R(t)]\frac{d\langle\Delta\hat{r}\rangle}{dt}. \tag{56}$$

By the Ehrenfest theorem [Eq. (50)] the $\langle\hat{p}_r\rangle$ and $\langle\Delta\hat{r}\rangle$ equations of motion are analogous to the classical mechanical expressions, from which a quasiclassical Langevin equation [Eq. (51)] may be derived using the linear response ansatz. The essence of Eq. (56) is that energy dissipation of a quantum oscillator subject to the mean field Ehrenfest equations of motion is connected to the frictional response of the classical bath to the motion of the quantum wave packet represented by the expectation value of momentum (and position) only.

In the classical path method the classical subsystem monitors the state of the quantum system through an expectation value, namely, the Hellmann-Feynman force of Eq. (18). As a result, an excess energy of the quantum subsystem, encoded in the wave function, is detected by the classical environment only to the extent that it expresses itself by way of a nonstationarity of the Hellmann-Feynman force under the action of the system Hamiltonian $\hat{H}_S$. A coherent state of the harmonic oscillator is a Gaussian wave packet of minimum uncertainty, where the expectation values of position and momentum, which move as their classical counterparts as stated by the Ehrenfest theorem, Eq. (50), completely define the expectation value of energy in terms of the coherent state parameter $\alpha(t)$, Eqs. (48) and (49). In this sense, a coherent state wave function of the HO represents a quasiclassical quantum state. It therefore seems natural to define, for an arbitrary quantum state of the harmonic oscillator, a reference coherent state that has the same expectation values of position and momentum associated with it as the actual wave packet,

$$\alpha_{\mathrm{ref}}(t) \equiv \frac{1}{\sqrt{2}} \left\{ \sqrt{\frac{\mu\omega_0}{\hbar}} \langle \Delta\hat{r} \rangle + i \frac{\langle \hat{p}_r \rangle}{\sqrt{\mu\hbar\omega_0}} \right\}. \tag{57}$$

The reference energy calculated from these expectation values, $\langle \hat{n} \rangle_{\mathrm{ref}}(t) \equiv |\alpha_{\mathrm{ref}}(t)|^2$, then corresponds to that part of the actual mean energy, which is detected by the classical environment. The remaining part, $\Delta\langle \hat{n} \rangle_{\mathrm{inert}} \equiv \langle \hat{n} \rangle(t) - \langle \hat{n} \rangle_{\mathrm{ref}} = \mathrm{const}$, is ''inert'' with respect to energy dissipation in a classical bath and therefore contributes to an *effective* zero point energy.

For a coherent state, the reference state is identical to the actual state, i.e., $\Delta\langle \hat{n} \rangle_{\mathrm{inert},\alpha} \equiv 0$. In the initial eigenstate case (quantum number n_0), $\langle \hat{n} \rangle_{\mathrm{ref},n_0}(t=0) \equiv 0$. Therefore, the total initial mean energy is inert, $\Delta\langle \hat{n} \rangle_{\mathrm{inert},n_0} \equiv \langle \hat{n} \rangle_{n_0}(t=0) = n_0$, and the initially occupied eigenstate is identical to the *effective* zero point level. As mentioned earlier, this is evident from the behavior of individual quantum/classical trajectories, subject to the mean field equations of motion.

In our simulations starting from an intermediate superposition state,

$$|\varphi_S(t=0)\rangle = \sqrt{\tfrac{1}{4}}|n_0-1\rangle + \sqrt{\tfrac{1}{2}}|n_0\rangle + \sqrt{\tfrac{1}{4}}|n_0+1\rangle,$$

$$\alpha_{\mathrm{ref}}(t=0) = \frac{1}{2}\left\{ \sqrt{\frac{n_0}{2}} + \sqrt{\frac{n_0+1}{2}} \right\} \simeq 1.657,$$

$$\langle \hat{n} \rangle_{\mathrm{ref}}(t=0) = \tfrac{1}{4}\{n_0 + \tfrac{1}{2} + \sqrt{n_0(n_0+1)}\} \simeq 2.744, \quad n_0 = 5,$$

and the *inert* part of the mean occupation number is $\Delta\langle \hat{n} \rangle_{\mathrm{inert}} = n_0 - \langle \hat{n} \rangle_{\mathrm{ref}}(t=0) \simeq 2.256$. This is *almost exactly* the lower bound of mean energy which is observed for individual quantum/classical trajectories starting from the intermediate superposition state.

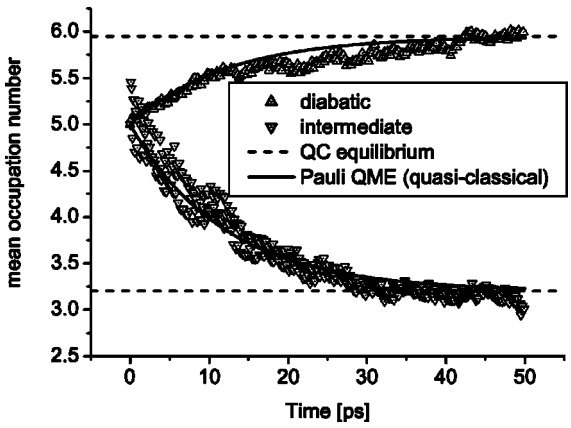

FIG. 12. Initial eigenstate and intermediate initial state energy relaxation towards quantum/classical equilibrium (see Table III) as compared to quasiclassical Pauli QME simulation ($\tau = \tau_{\mathrm{cl}}, \overline{n} = k_B T/\hbar\omega_0$).

In Fig. 12 we analyze the decay of ensembles of initial eigenstates and intermediate coherences, respectively, towards the assumed quantum/classical equilibrium introduced above, i.e., $\langle \hat{n} \rangle \to n_0 + k_B T/\hbar\omega_0$ and $\langle \hat{n} \rangle \to \Delta\langle \hat{n} \rangle_{\mathrm{inert}} + k_B T/\hbar\omega_0$. In both cases, relaxation is exponential to a good approximation, where the relaxation time obtained for the intermediate initial state case is reasonably close to the classical energy relaxation time (Table III). The diabatic initial state case can be understood in terms of a quasiclassical heating of an initially ''cold'' oscillator induced by the classical bath. The numerically obtained relaxation time, however, is too large as compared to τ_{cl}. The question, whether this is merely a result of limited statistics or resultant from the effect of the delocalized wave function upon the Hellmann-Feynman force $F_R^{\mathrm{HF}} = -\langle \nabla_R \hat{H}_{SB}[R(t)] \rangle$, must be left open. Comparison to the result of a quasiclassical Pauli QME simulation ($\tau = \tau_{\mathrm{cl}}$, $\overline{n} = k_B T/\hbar\omega_0$, Fig. 12) taking account of the inert part of vibrational excess energy, however, suggests that both diabatic and intermediate initial state energy relaxation within the QCMD approximation are consistent with a quasiclassical picture of the relaxation process, while statistical convergence has not yet been achieved.

Let us note here that our procedure of defining ''quasiclassical'' and ''quantum'' parts of the mean energy of a quantum oscillator can at most be approximately applicable only, because the classical bath does not ''observe'' the expectation value of the HO displacement but the expectation value of $\hat{F}_R^e = -\nabla_R \hat{H}_{SB}[R(t)]$, which may only approximately be linear in $\Delta\hat{r}$.

F. Approach to quasicanonical equilibrium

In the preceding section we have seen that the mean energy relaxation of a quantum oscillator in a classical bath subject to the classical path equations of motion can be understood in terms of a quasiclassical relaxation, where only a fraction of the total mean energy, which is ''stored'' quasiclassically in the evolving quantum wave packet, is subject to dissipation and fluctuation in a classical environment.

On the level of diabatic state populations, the quasiclassical relaxation process just described quite obviously cannot lead to a canonical structure of the equilibrium level distri-

butions for arbitrary quantum initial states. When part of the quantum mean energy is inert, and therefore contributes to the *effective* zero point energy (ZPE) under the mean field quantum/classical EOM, the populations of levels below the effective ZPE do not lend themselves to a proper physical interpretation. This is immediately evident in the diabatic initial state case (Fig. 6 in Sec. IV B). However, even for an intermediate superposition state, where part of the total mean energy is inert towards dissipation, the final equilibrium distribution closely resembles a canonical one (Fig. 6).

In this section, we investigate the approach to quantum/classical equilibrium by exploiting the special properties of the harmonic oscillator equilibrium distribution function. As a global measure of the evolving quantum state distribution $\{p_n\}$ we use the nonequilibrium (information) entropy

$$S(t) = -\sum_n p_n \ln p_n \equiv \ln N_{\mathrm{eff}}(t) \tag{58}$$

defined in terms of the dynamically evolving diabatic state populations $p_n(t) = \rho_{nn}(t)$, instead of using $S(t) = -\mathrm{Tr}\{\hat{\rho}_S \ln \hat{\rho}_S\}$ [39,42]. The identity $S(t) = \ln N_{\mathrm{eff}}(t)$ is employed for the sake of an intuitive physical picture of the nonequilibrium entropy, defining a reference distribution where N_{eff} states are equally populated. At canonical equilibrium characterized by the temperature parameter $\beta = 1/k_B T$, the populations of HO energy eigenstates are given by [39]

$$p_n = \left(\frac{\overline{n}}{\overline{n}+1}\right)^n \frac{1}{\overline{n}+1} = e^{-n\beta\hbar\omega_0}\{1 - e^{-\beta\hbar\omega_0}\}, \tag{59}$$

where $\overline{n}$ is the mean thermal occupation number. Note that at quantum/classical equilibrium $\overline{n}$ has to be replaced by its classical limit. Due to the specific dependence of p_n on $\overline{n}$ at canonical equilibrium, the information entropy may be solely expressed in terms of the mean occupation number,

$$S_{\mathrm{canonical}}(t) = (\langle \hat{n} \rangle + 1)\ln(\langle \hat{n} \rangle + 1) - \langle \hat{n} \rangle \ln \langle \hat{n} \rangle,$$

$$N_{\mathrm{canonical}}(t) = \frac{(\langle \hat{n} \rangle + 1)^{\langle \hat{n} \rangle + 1}}{\langle \hat{n} \rangle^{\langle \hat{n} \rangle}}, \tag{60}$$

where we have replaced the stationary value $\overline{n}$ by its dynamic analogue $\langle \hat{n} \rangle$. Thus, whenever the exact information entropy, in terms of state populations, is equal or close to the canonical reference entropy, given in terms of the mean occupation number, may we assign an effective temperature to the relaxing ensemble, where $\langle \hat{n} \rangle$ may or may not be stationary. The relaxation towards a quasicanonical distribution can be described via the decay of $\Delta S(t) \equiv S(t) - S_{\mathrm{canonical}}(t)$ or $\Delta N_{\mathrm{eff}}(t) \equiv N_{\mathrm{eff}}(t) - N_{\mathrm{canonical}}(t)$.

Figures 13(a) QCMD, 13(b) Pauli QME treatment, and 14 show the relaxation of level distributions $\{p_n\}$ towards quasicanonical equilibrium for quantum/classical ensembles of coherent and intermediate initial states, respectively. While the time scales are approximately equal in both cases ($\tau \simeq 4.5$ ps), we note that only in the coherent state case a numerically exact equivalence to a canonical distribution is obtained at long times. In the intermediate superposition state case a small but notable difference between exact and canonical reference distributions remains even at long times. This is in accord with our notions stated above regarding the nature of quantum/classical equilibrium for arbitrary quantum initial states.

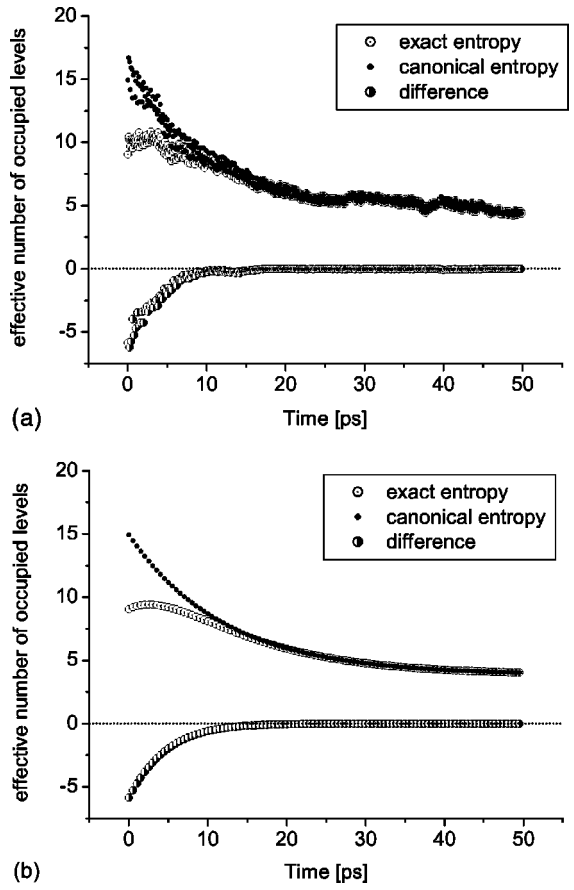

FIG. 13. Approach to quasicanonical equilibrium for coherent initial state; (a) QCMD results, (b) quasiclassical Pauli QME simulation.

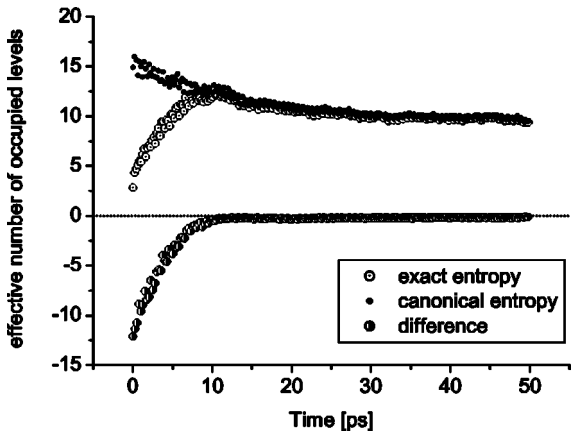

FIG. 14. The same as Fig. 13, but for intermediate initial state (QCMD results only).

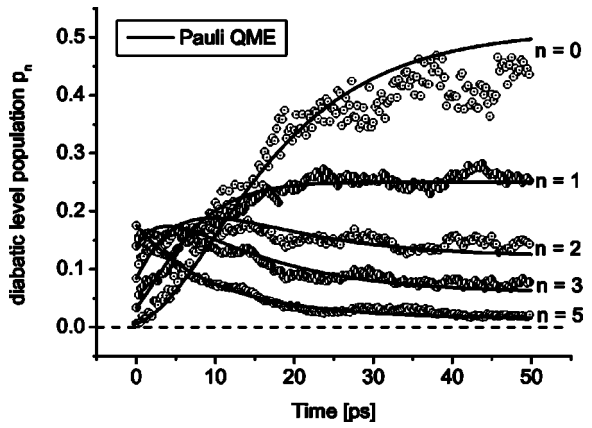

FIG. 15. Time evolution of diabatic state populations for coherent initial state as compared to a quasiclassical QME simulation [$\overline{K}=\overline{K}_{\mathrm{cl}}$, $\overline{n}=k_BT/\hbar\omega_0$; see Fig. 13(b)].

In Fig. 15 we compare the decay of level populations for the coherent state case obtained by QCMD and by a Pauli master equation treatment, where—as in Fig. 13(b)—the average relaxation rate $\overline{K}$ as well as the mean thermal occupation number $\overline{n}$ have been replaced by their classical limits. The agreement underscores the quasiclassical nature of the relaxation process.

V. CONCLUSION

In the present work, we have reported on nonequilibrium hybrid quantum/classical simulations of the liquid state vibrational energy relaxation, using a simple model Hamiltonian that captures the essential features of diatomic vibrational relaxation in liquids while rigorously excluding vibration-rotation pathways of vibration to solvent energy flow. The general aim of this work is to test the performance and statistical mechanical properties of the mean field Ehrenfest quantum/classical method for different quantum initial conditions, i.e., coherent vs delocalized (diabatic eigenstate) wave packets, thereby probing the degree of dynamic correlation between quantum and classical subsystems dependent on the shape of the evolving wave function. Fully classical simulations are used as a reference, assuming that the classical rate of relaxation may be used to estimate the exact quantum rate.

Among the various possible quantum initial state vectors at a given mean vibrational energy, coherent states and eigenstates of the harmonic oscillator represent wave functions of extremely different character. Coherent states are the most classical-like quantum states that may be constructed. Eigenfunctions of the HO Hamiltonian, however, do not possess a classical analog.

While coherent states relax towards a quasiclassical thermal equilibrium, defined by the bath temperature and the classical limit of the mean thermal occupation number, eigenstates experience unphysical heating towards a stationary state where the classical mean thermal energy k_BT has been added on top of the initial vibrational energy. An arbitrary superposition state intermediate between the coherent state and eigenstate limits relaxes towards a stationary ensemble, where only part of the initial excess energy has been dissipated into the classical bath.

In order to provide a basis for the rationalization of physical artifacts produced by the mean field quantum/classical equations of motion, two limiting theoretical cases have been examined: (i) the complete breakdown of detailed balance using a Pauli master equation analysis and (ii) the relaxation of a coherent state wave packet using a quantum/classical Langevin equation (LE) derived from the QCMD equations of motion.

The results show that a complete breakdown of detailed balance, leading to a linear energy increase induced by the classical bath fluctuations, is not an adequate model for understanding the initial eigenstate case. Rather, an initial eigenstate is driven into a coherence via the system-bath interaction, thereby increasing the system-bath correlation in a classical dynamical sense, which in turn leads to a controlled energy growth. The quantum/classical Langevin equation, on the other hand, adequately describes the quasiclassical relaxation of an ensemble of coherent initial states.

The success of the quantum/classical LE ansatz points towards a general concept for rationalizing the behavior of arbitrary quantum initial states subject to the mean field Ehrenfest equations of motion. The self-consistent coupling between the motion of quantum and classical subsystems suffers from an imbalance in the bidirectional energy flow. While the quantum system is driven by a time-dependent interaction operator determined by the positions of classical particles, the motion of the classical degrees of freedom is affected by a quantum-averaged Hellmann-Feynman force, i.e., an expectation value calculated from the quantum wave packet. As a result, the classical subsystem is correlated to the evolving quantum state vector only to the extent that the Hellmann-Feynman force is nonstationary under the action of the bare system Hamiltonian. From a statistical mechanical perspective, a breakdown of the quantum detailed balance relationship emerges. However, this breakdown is not complete and depends on the shape of the quantum wave packet. From the time derivative of the vibrational energy expectation value $\langle\hat{H}_S\rangle$, accompanied by the Ehrenfest theorem, it can be shown that within the limits of linear response energy dissipation subject to mean field QCMD is connected to the frictional response of the classical bath to the expectation value of vibrational momentum. In other words, a classical-like fluctuation-dissipation theorem holds. As a result, for an arbitrary vibrational quantum initial state, the mean energy may be divided into two parts, one which is encoded quasiclassically in terms of the nonstationarity of position and momentum expectation values, and one which is encoded in the nodal structure of the wave function (in position space). A classical bath is within the mean field QCMD method only correlated to the ''classical'' part of the mean energy. The remaining ''quantum'' part of the excess energy is inert towards dissipation and fluctuation and therefore contributes to an effective zero point energy.

It has become clear from our investigations that the MF Ehrenfest quantum/classical method is not reliable for the simulation of condensed phase vibrational energy relaxation,

starting from arbitrary quantum initial states. While the general notion of a (partial) breakdown of detailed balance subject to the classical path EOM is not unanticipated (e.g., Refs. [2,18]), we believe that our results provide some insight that may serve as a basis for developing adequate quantum/classical approaches to the liquid state vibrational energy transfer. The general strategy for improving direct quantum/classical approaches to liquid phase VER beyond the simple mean field Ehrenfest ansatz therefore demands an increase of correlation between subsystems, either within the TDSCF approximation or starting from more rigorous multiconfiguration (MC) treatments. Apart from making a distinction between single-configuration and MC-TDSCF approaches, increase of correlation may be achieved either by introducing ''classical'' features, i.e., stochastic ''quantum jumps,'' into the quantum time evolution of the system or by introducing approximate quantum (semiclassical) effects into the evolution of the bath degrees of freedom. From a different perspective, the quantum/classical Langevin equation derived in this paper may serve as a starting point for a stochastic Hamiltonian approach to the problem at hand. Work along these lines is currently in progress in our laboratory.

ACKNOWLEDGMENTS

This work was made possible by a generous funding of computing facilities in our department by the Max-Planck-Gesellschaft. The author is grateful to Professor Jürgen Troe for his continuous support, as well as to Dr. Jörg Schroeder, Dr. Dirk Schwarzer and Dr. Anatol Neufeld for helpful discussions. D. Schwarzer also took part in this project in doing classical dynamical reference simulations. We would also like to thank Professor Christof Schütte and Dr. Burkhard Schmidt for introducing us to their PICKAPACK algorithm. The help of Dr. Reinhard Schinke and especially Dr. Sergy Grebenshchikov in discussing and implementing a DVR version of the PICKAPACK algorithm is hereby gratefully acknowledged. Last but not least, the author expresses his gratitude to Professor Gert D. Billing for the hospitality during a short visit at the H.C. Ørsted Institute, University of Copenhagen, where some of the present issues were discussed.

[1] *Classical and Quantum Dynamics in Condensed Phase Simulations*, edited by B. J. Berne, G. Ciccotti, and D. F. Coker (World Scientific, Singapore, 1998).
[2] G. D. Billing, in *Encyclopedia of Computational Chemistry*, edited by P. von R. Schleyer (Wiley, New York, 1998), p. 1587.
[3] J. C. Tully, in *Modern Methods for Multidimensional Dynamics Computations in Chemistry*, edited by D. L. Thompson (World Scientific, Singapore, 1998), p. 34; Faraday Discuss. **110**, 407 (1998).
[4] S. Hammes-Schiffer, J. Phys. Chem. A **102**, 10 443 (1998).
[5] K. Drukker, J. Comput. Phys. **153**, 225 (1999).
[6] P. Jungwirth and R. B. Berber, Chem. Rev. **99**, 1583 (1999).
[7] N. Makri, Annu. Rev. Phys. Chem. **50**, 167 (1999).
[8] W. H. Miller, J. Phys. Chem. A **105**, 2942 (2001).
[9] W. Domcke and G. Stock, Adv. Chem. Phys. **100**, 1 (1997).
[10] D. F. Coker and L. Xiao, J. Chem. Phys. **102**, 496 (1995).
[11] E. J. Heller, J. Phys. Chem. A **103**, 10 433 (1999).
[12] N. Makri, J. Phys. Chem. A **102**, 4414 (1998).
[13] R. B. Gerber and M. A. Ratner, Adv. Chem. Phys. **70**, 97 (1988).
[14] R. B. Gerber *et al.*, in *Modern Methods for Multidimensional Dynamics Computations in Chemistry*, edited by D. L. Thompson (World Scientific, Singapore, 1998), p. 238.
[15] D. Kohen, F. H. Stillinger, and J. C. Tully, J. Chem. Phys. **109**, 4713 (1998).
[16] J. C. Tully, J. Chem. Phys. **93**, 1061 (1990).
[17] S. Hammes-Schiffer and J. C. Tully, J. Chem. Phys. **101**, 4657 (1994).
[18] G. D. Billing, Int. Rev. Phys. Chem. **13**, 309 (1994).
[19] (a) C. B. Harris, D. E. Smith, and D. J. Russell, Chem. Rev. **90**, 481 (1990); (b) J. C. Owrutsky, D. Raftery, and R. M. Hochstrasser, Annu. Rev. Phys. Chem. **45**, 519 (1994); (c) D. W. Oxtoby, Adv. Chem. Phys. **47**, 487 (1981); (d) D. W. Oxtoby, Annu. Rev. Phys. Chem. **32**, 77 (1981); (e) J. Chesnoy and G. M. Gale, Ann. Phys. (Paris) **9**, 893 (1984); (f) J. Chesnoy and G. M. Gale, Adv. Chem. Phys. **70**, 297 (1988); (g) S. A. Adelman *et al.*, *ibid.* **84**, 73 (1993); (h) D. W. Miller and S. A. Adelman, Int. Rev. Phys. Chem. **13**, 359 (1994); (i) R. M. Stratt and M. Maroncelli, J. Phys. Chem. **100**, 12 981 (1996).
[20] S. A. Egorov, E. Rabani, and B. J. Berne, J. Phys. Chem. B **103**, 10 978 (1999); S. A. Egorov and B. J. Berne, J. Chem. Phys. **107**, 6050 (1997).
[21] G. Käb and V. S. Vikhrenko, Phys. Chem. Chem. Phys. **3**, 2223 (2001).
[22] G. Käb, C. Schröder, and D. Schwarzer, Phys. Chem. Chem. Phys. **4**, 271 (2002).
[23] S. Okazaki, Adv. Chem. Phys. **118**, 191 (2001).
[24] T. Terashima, M. Shiga, and S. Okazaki, J. Chem. Phys. **114**, 5663 (2001).
[25] S. Jang, Y. Pak, and G. A. Voth, J. Phys. Chem. A **103**, 10 289 (1999).
[26] M. H. Beck *et al.*, Phys. Rep. **324**, 1 (2000).
[27] A. Raab, Chem. Phys. Lett. **319**, 674 (2000).
[28] G. D. Billing and K. V. Mikkelsen, *Advanced Molecular Dynamics and Chemical Kinetics* (Wiley, New York, 1997).
[29] H. Hellmann, Z. Phys. **85**, 180 (1933).
[30] R. P. Feynman, Phys. Rev. **56**, 340 (1939).
[31] H. Jiang and X. S. Zhao, J. Chem. Phys. **113**, 930 (2000).
[32] P. Nettesheim *et al.*, Chem. Phys. Lett. **256**, 581 (1996).
[33] F. A. Bornemann, P. Nettesheim, and C. Schütte, J. Chem. Phys. **105**, 1074 (1996).
[34] V. S. Vikhrenko *et al.*, J. Chem. Phys. **110**, 5273 (1999).
[35] G. C. Schatz and M. A. Ratner, *Quantum Mechanics in Chemistry* (Prentice-Hall, Englewood Cliffs, NJ, 1993).
[36] S. A. Egorov and J. L. Skinner, J. Chem. Phys. **112**, 275 (2000).
[37] Q. Liu, J.-K. Wang, and A. H. Zewail, J. Phys. Chem. **99**, 11 321 (1995).

[38] J. K. Johnson, J. A. Zollweg, and K. E. Gubbins, Mol. Phys. **78**, 591 (1993).
[39] C. W. Gardiner and P. Zoller, *Quantum Noise* (Springer, Berlin, 2000).
[40] V. May and O. Kühn, *Charge and Energy Transfer Dynamics in Molecular Systems* (Wiley-VCH, Berlin, 2000).
[41] D. W. Oxtoby, Adv. Chem. Phys. **47**, 487 (1981).
[42] R. Kubo, M. Toda, and N. Hashitsume, *Statistical Physics II* (Springer, Berlin, 1991).
[43] P. Ehrenfest, Z. Phys. **45**, 455 (1927).